Enhancement of Imprinting Effect in Ferroelectric AlScN Films for Non-Destructive Capacitive Readout Operation Using Metal-Capping Oxidation (MCO) Process

Shun Komai[1*], Si-Meng Chen[1], Takuya Hoshii[1],
Kazuo Tsutsui[2], Hitoshi Wakabayashi[2], and Kuniyuki Kakushima[1]
[1]School of Engineering, [2]Institute of Integrated Research, Institute of Science Tokyo, Yokohama, Japan
*Email: komai.s.f1b3@m.isct.ac.jp

1. Introduction

The concept of capacitive readout for ferroelectric (FE) memory technology has recently drawn considerable attention for non-volatile memory (NVM) [1]. Unlike the traditional switching-driven readout scheme [2], the capacitive readout features lower power consumption and non-destructive data sensing, which alleviates the burden on endurance strength. However, the key to realizing capacitive readout is that the memory window (MW), i.e., high/low capacitance gap at 0 V, should be sufficiently wide. Although some experimental demonstrations have been conducted with HfO_2-based FE materials [3-4], research works with capacitive readout are still lacking for nitride FE materials such as AlScN. With a lower relative permittivity (ε_r) of 11-19, AlScN holds a great advantage over HfO_2-based and lead zirconium titanate (PZT) FE materials with this scheme. Herein, we propose a simple metal-capping oxidation (MCO) process for AlScN thin films with enhanced MW, thereby unlocking their potential for capacitive readout operation.

2. Experimental Methods

The structural diagram and process flow of AlScN capacitors are shown in Figs. 1(a) and 1(b), respectively. The experimental procedures are similar to our previous work [5], except that we fabricated two FE layer thicknesses (25 and 50 nm). Additionally, we deployed the MCO process before top electrode deposition to indirectly oxidize the FE layer [6], as described below. After FE deposition, a 3-nm W layer was capped on the FE layer and followed by rapid thermal annealing (RTA) in O_2 ambient for 30 min at 400°C, which transforms metal W to dielectric WO_x.

3. Results and Discussion

Fig. 2 depicts the polarization-electric field (P-E) hysteresis and current density-electric field (J-E) curves for all capacitors, validating the FE characteristics. However, due to leakage current, positive-up negative-down (PUND) was deployed, as displayed in Figs. 3(a) and 3(b). For 50-nm FE films, P_r is enhanced at higher fields and exhibits good semi-saturation by the MCO process. Similarly, for 25-nm FE films, considerably enhanced P_r shows that the MCO process could compensate for the deficit of worse crystallinity in thinner films [7], and thereby reaching 191 $\mu C/cm^2$ in maximum. Moreover, a slight increase in E_c values is observed in MCO-treated capacitors, as plotted in Fig. 3(c). Fig. 4 plots the leakage and breakdown characteristics for all capacitors in the as-deposited state. Leakage suppression and breakdown field (E_{BD}) improvements are observed in MCO cases, though the source of contribution still remains to be distinguished. Involvement of the dielectric WO_x layer or partially oxidized AlScN FE layer could be the origin. Additionally, the switching event becomes more pronounced for MCO capacitors, indicating that the initial N-polar state can be partially inverted by extrinsic oxidation, in addition to incorporation of oxygen atoms during AlScN deposition [8].

Fig. 5 displays the butterfly-shaped capacitance-electric field (C-E) curves. Overall, ε_r is generally decreased with the MCO process, which is attributed to the insertion of a thin dielectric WO_x layer. The permittivity at the cross-point (ε_i) is extracted and plotted in Fig. 6(a). The imprint effect is visable with MCO process, as ε_i values shift toward negative, and possibly due to high defect density at the oxide/nitride interface. For capacitive readout, the MW is defined here as ΔC and ΔC^*, respectively, for as-deposited and 100-cycle-switched capacitors, as indicated in Fig. 5(d). With the MCO process, ΔC is significantly increased for both 25 nm and 50 nm capacitors. Furthermore, ΔC^* also demonstrated robustness against write operations. It is speculated that the uprising ΔC and ΔC^* with MCO process are related to a modified switching mechanism by graded oxidization of FE AlScN. Nonetheless, ~4.2× enhancement of ΔC and ΔC^* is demonstrated, as summarized in Fig. 6(b).

4. Conclusions

In this work, we study the utilization of the MCO process in FE AlScN thin films to unlock the potential of non-destructive capacitive readout in nitride FE materials. The results indicate that MCO not only boosts P_r performance but also suppresses leakage current while enhancing E_{BD}. Owing to the thin dielectric WO_x layer, ε_r is found to be slightly decreased along with more pronounced imprint effects. Most importantly, MCO-treated FE AlScN films exhibit ~4.2× increment of MW at zero electric field, which is beneficial for capacitive readout operation in future NVM technologies.

Acknowledgements

This work is supported by the MEXT Initiative to Establish Next-generation Novel Integrated Circuits Centers (X-NICS) Grant Number JPJ011438.

References

[1] J. Hur *et al.*, Adv. Intell. Syst. **4**, 2100258 (2022). [2] A. Sheikholeslami *et al.*, Proc. IEEE **88**, pp. 667-689 (2000). [3] S. Mukherjee *et al.*, IEEE Electron Device Lett. **44**, pp. 1092-1095 (2023). [4] S. Wu *et al.*, Appl. Phys. Lett. **124**, 102902 (2024). [5] S.-M. Chen *et al.*, IEEE Electron Device Lett. **45**, pp. 2090-2093 (2024). [6] E. Cartier *et al.*, Appl. Phys. Lett. **95**, 042901 (2009). [7] R. Mizutani *et al.*, Appl. Phys. Express **14**, 105501 (2021). [8] M.R. Islam *et al.*, Adv. Electron. Mater **11**, 2400874 (2025).

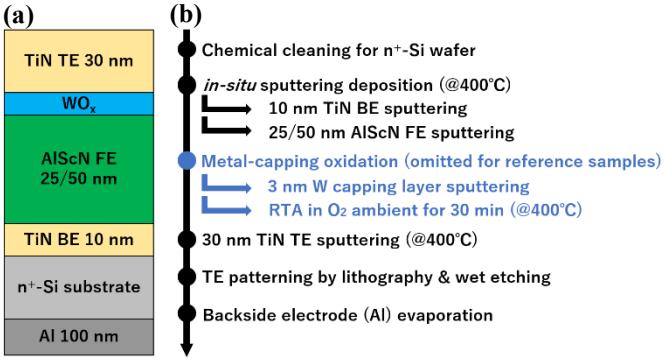

Fig. 1 (a) Schematic diagram and (b) process flow of fabricated AlScN capacitors.

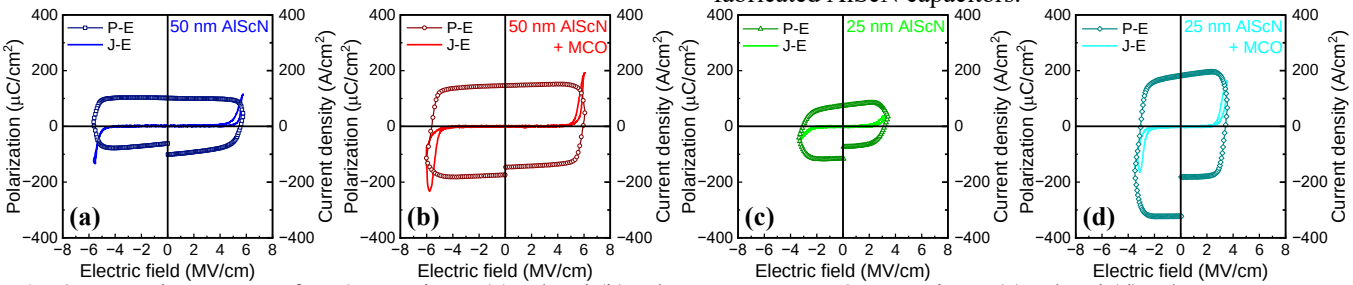

Fig. 2 P-E and J-E curves for 50 nm AlScN (a) w/ and (b) w/o MCO process; 25 nm AlScN (c) w/ and (d) w/o MCO process.

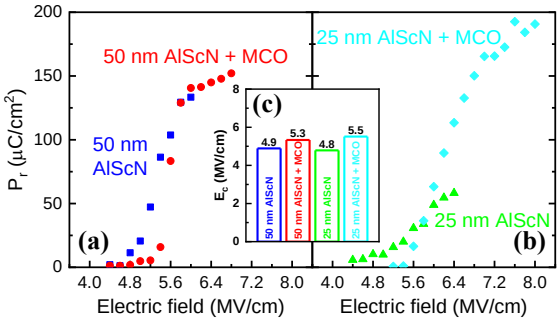

Fig. 3 PUND results for (a) 50 nm and (b) 25 nm capacitors. (c) E_c extracted by linear extrapolation from PUND [5].

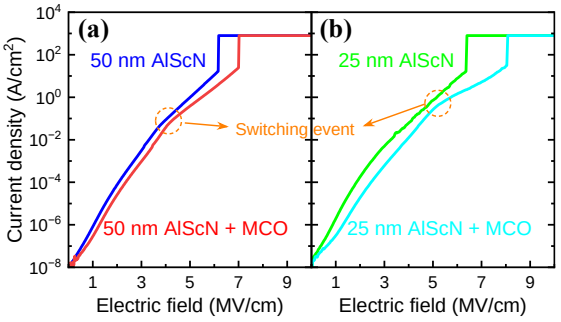

Fig. 4 Leakage and breakdown characteristics for (a) 50 nm and (b) 25 nm capacitors.

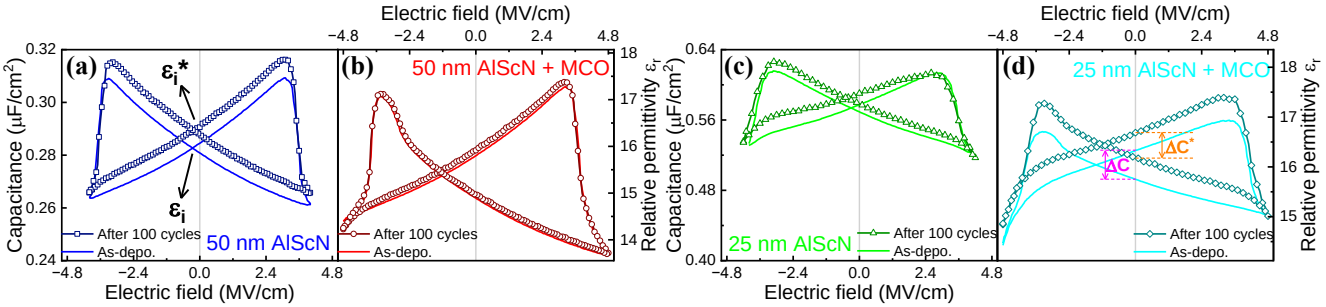

Fig. 5 Butterfly-shaped C-E curves for 50 nm AlScN (a) w/ and (b) w/o MCO process; 25 nm AlScN (c) w/ and (d) w/o MCO process. Solid lines and scattered points represent data from as-deposited and 100-cycle-switched capacitors.

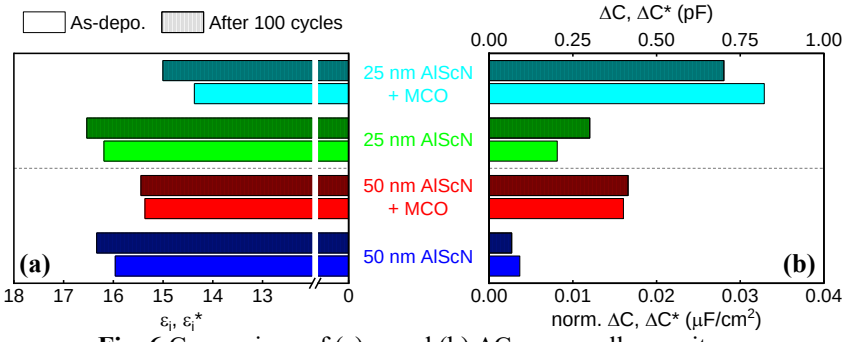

Fig. 6 Comparison of (a) ε_i and (b) ΔC among all capacitors.